

# KINETIC MODELING OF ELECTRO-FENTON REACTION IN AQUEOUS SOLUTION

H. Liu<sup>1</sup>, X. Z. LI<sup>\*2</sup>, Y. J. Leng<sup>3</sup>, C. Wang<sup>1</sup>

<sup>1</sup>*School of Chemistry and Chemical Engineering, Sun Yat-sen University, Guangzhou, 510275, China.*

<sup>2</sup>*Department of Civil and Structural Engineering, The Hong Kong Polytechnic University, Hong Kong, China*

<sup>3</sup>*School of Mechanical and Aerospace Engineering, Nanyang Technological University, 50 Nanyang Ave, Singapore 639798*

## Abstract

To well describe the electro-Fenton (E-Fenton) reaction in aqueous solution, a new kinetic model was established according to the generally-accepted mechanism of E-Fenton reaction. The model has special consideration on the rates of hydrogen peroxide (H<sub>2</sub>O<sub>2</sub>) generation and consumption in the reaction solution. The model also embraces three key operating factors affecting the organic degradation in the E-Fenton reaction, including current density, dissolved oxygen concentration and initial ferrous ion concentration. This analytical model was then validated by the experiments of phenol degradation in aqueous solution. The experiments demonstrated that the H<sub>2</sub>O<sub>2</sub> was gradually built up with time and eventually approached its maximum value in the reaction solution. The experiments also showed that phenol was degraded at a slow rate at the early stage of the reaction, a faster rate during the middle stage, and a slow rate again at the final stage. It was confirmed in all experiments that the curves of phenol degradation (concentration vs. time) appeared to be an inverted “S” shape. The experimental data were fitted using both the normal first-order model and our new model, respectively. The goodness of fittings demonstrated that the new model could better fit the experimental data in all experiments than the first-order model appreciably, which indicates that this analytical model can better describe the kinetics of the E-Fenton reaction mathematically and also chemically.

**Keywords:** E-Fenton; H<sub>2</sub>O<sub>2</sub>; Kinetic Model; Phenol

---

\* Corresponding author, Tel.: (852) 2766 6016; Fax: (852) 2334 6389; Email address: cexzli@polyu.edu.hk

## 29 **1. Introduction**

30

31 It has been well proven that a variety of refractory organics can be effectively degraded by the  
32 Fenton reaction without producing any toxic substances in water environment (Joseph, 1992;  
33 Oliveros et al., 1997; Lunar et al., 2000; Kawabe et al., 2004; Wang et al., 2004). Recent  
34 development of electro-Fenton (E-Fenton) reaction by generating  $H_2O_2$  from dissolved oxygen in  
35 aqueous solution electrically provides fresh  $H_2O_2$  in a continuous mode, which is more efficient and  
36 cost-effective than conventional chemical dosing methods (Brillas et al., 1998; Brillas et al., 2000;  
37 Brillas and Casado, 2002; Brillas et al., 2003; Gözmen et al., 2003).

38 It should be noted that like most chemical reactions, the  $H_2O_2$  concentration in a conventional  
39 Fenton reaction is gradually reduced after a batch chemical dosing along with reaction time (Malato  
40 et al., 2001; Liu et al., 2003). It has been reported that adding  $H_2O_2$  in a single batch leaves much of  
41 it available to attack by hydroxyl radicals, whereas continuously feeding smaller quantities of the  
42 reagent to the system would allow the majority of radicals generated to target the organic  
43 contaminant (Duesterberg and Waite, 2006). In an E-Fenton reaction process,  $H_2O_2$  is continuously  
44 generated on the cathode throughout the reaction and its accumulative concentration in aqueous  
45 solution depends on a competition between its generation rate and consumption rate (Oturán, 2000;  
46 Oturán et al., 2000; Boye et al., 2002). Particularly, at the beginning of the reaction such as the first  
47 5 min, the  $H_2O_2$  concentration rises from zero and the rate of organic degradation in aqueous  
48 solution is quite slow, although  $H_2O_2$  concentration builds up at a maximum rate. When the reaction  
49 further proceeds, the rate of organic degradation is gradually increased with the increased  $H_2O_2$   
50 concentration and then eventually decreased again. Therefore, the most commonly-used first-order  
51 reaction model has a difficulty to well describe the kinetics with a continuous  $H_2O_2$  supply,  
52 particularly during the initial reaction period of the E-Fenton reaction (Malato et al., 2001; Gözmen  
53 et al., 2003). Wang and Lemley in 2001 developed a second-order kinetic model to describe the  
54 E-Fenton reaction (anodic Fenton reaction) for degradation of 2,4-dichlorophenoxyacetic acid in  
55 aqueous solution as a more accurate kinetic model than the first-order model. Moreover, a recent  
56 work by Anota et al. in 2006 compared the kinetics of aniline degradation by Fenton and E-Fenton  
57 reactions. It was found that the overall rate equation for aniline degradation by Fenton reaction  
58 followed a reaction order of 1.1 (almost a first-order reaction), but that by E-Fenton reaction

59 demonstrated a reaction order of 0.46 (about a half-order reaction). Alternatively, other researchers  
60 still applied the first-order model to describe the E-Fenton reaction but either in terms of total  
61 organic carbon (Brillas et al., 1998; Brillas et al., 2000) or by subdividing the overall reaction  
62 period into two or three phases with different values of kinetic constant representing different  
63 reaction rates (Chu et al., 2005). It should be indicated that a good kinetic model to well describe  
64 the E-Fenton reaction should consider some other key factors including current density, dissolved  
65 oxygen concentration and ferrous ion concentration jointly.

66 In this work, a new kinetic model for the E-Fenton reaction in aqueous solution was established  
67 according to the generally-accepted mechanism of the E-Fenton reaction. Phenol was used as a  
68 model pollutant and a series of phenol degradation experiments in an E-Fenton reaction system  
69 were carried out. The new model was then validated by the experimental data and evaluated in this  
70 study.

71

## 72 **2. Experimental Section**

73

### 74 *2.1. Chemicals*

75

76 Phenol, hydrogen peroxide ( $\text{H}_2\text{O}_2$ , 30% w/v), sodium sulfate ( $\text{Na}_2\text{SO}_4$ ), potassium titanium (IV)  
77 oxalate [ $\text{K}_2\text{Ti}(\text{C}_2\text{O}_4)_3$ ] and ferrous sulfate ( $\text{FeSO}_4 \cdot 7\text{H}_2\text{O}$ ) chemicals were obtained from Aldrich,  
78 USA with analytical grade and used without further purification.

79

### 80 *2.2. Experimental setup*

81

82 All experiments were conducted in an E-Fenton reactor consisting of two electrochemical cells  
83 connected with a glass frit. A Pt flake (20 mm  $\times$  20 mm) from Superior Chemicals & Instruments,  
84 China was used as the anode and a commercially-available carbon rod ( $\Phi = 5$  mm and L = 80 mm)  
85 from Shanghai, China was employed as the cathode to generate  $\text{H}_2\text{O}_2$ . In addition, a saturated  
86 calomel electrode was applied as the reference electrode. Both the cathode and the reference  
87 electrode are placed in one compartment, while the anode is placed in another compartment. A  
88 potentiostat/galvanostat (ZF-9) from Zhenfang Electronic Ltd., China was employed to apply an

89 electrical current between the anode and cathode. This E-Fenton reactor has an effective volume of  
90 150 mL. Phenol solution was prepared in aqueous 0.01 M Na<sub>2</sub>SO<sub>4</sub> electrolyte solution. The pH of  
91 reaction solution was adjusted to be 2.5 using 0.1 M H<sub>2</sub>SO<sub>4</sub> before reaction. A mixture gas of  
92 oxygen and air was continuously bubbled through a sintered-glass diffuser to supply dissolved  
93 oxygen and also to provide mixing, in which the concentrations of dissolved oxygen in the reaction  
94 solution were maintained at 0.26 mM, 0.40 mM and 0.57 mM, respectively in three sets of  
95 experiments, when different ratios between oxygen and air gases were controlled. During the  
96 reaction, water samples were collected at different time intervals for analyses. To quench any  
97 further reaction with radicals in the samples, 10 μL of methanol was injected into the 2.0 mL of  
98 sample as soon as the sample taking.

99

### 100 2.3. Analytical Methods

101

102 Phenol concentration was analyzed by HPLC (Waters 486) equipped with a reverse-phase column  
103 (Waters, XTerra™ MS C-18) and a UV detector. A mobile phase consists of acetonitrile and water  
104 (20%:80%) with 0.5% acetic acid. Under these conditions, phenol was determined at the  
105 wavelength of 269 nm with a retention time of 5.8 min. The ferrous ion (Fe<sup>2+</sup>) concentration was  
106 determined using a UV-VIS spectrophotometer (Spectronic, GENISIS-2), according to the light  
107 absorption at 510 nm of a colored complex solution formed from Fe<sup>2+</sup> and 1,10-phenanthroline  
108 (APHA, 1995). H<sub>2</sub>O<sub>2</sub> solution was prepared with 30% H<sub>2</sub>O<sub>2</sub> chemical and calibrated by KMnO<sub>4</sub>  
109 titration, which had been calibrated by Na<sub>2</sub>C<sub>2</sub>O<sub>4</sub> titration (Vogel, 1978). Whereas, the H<sub>2</sub>O<sub>2</sub>  
110 concentration during the E-Fenton reaction was determined using the UV-VIS spectrophotometer,  
111 according to the light absorption at 407 nm of a yellow complex solution formed from the H<sub>2</sub>O<sub>2</sub> and  
112 K<sub>2</sub>Ti(C<sub>2</sub>O<sub>4</sub>)<sub>3</sub> in 2 M H<sub>2</sub>SO<sub>4</sub> solution to prevent any interference caused by the organic disturbance  
113 (Sellers, 1980).

114

### 115 3. Kinetic Modeling of E-Fenton Reaction

116

117 It is generally believed that a typical E-Fenton reaction should involve three key reactions: (1) the  
118 generation of H<sub>2</sub>O<sub>2</sub> from dissolved oxygen on the surface of the cathode (Reaction 1), (2) the

119 generation of hydroxyl radicals ( $\cdot\text{OH}$ ) between  $\text{H}_2\text{O}_2$  and  $\text{Fe}^{2+}$  (Reaction 2), and (3) the degradation  
 120 of organic substance by the  $\cdot\text{OH}$  (Reaction 5). In the meantime, some reversed reactions and side  
 121 reactions (Reactions 3, 4, 6 and 7) coexist along with the key reactions as summarized below  
 122 (Walling, 1975; Buvet et al., 1987; Neyens and Baeyens, 2003);



130 To establish a new kinetic model for describing the E-Fenton reaction, we may assume that  
 131 organic substance (S) is primarily degraded by the  $\cdot\text{OH}$  and its reaction rate ( $\frac{d[S]}{dt}$ ) can be  
 132 expressed by Eq. 1:

133  
 134 
$$-\frac{d[S]}{dt} = k_5[\cdot\text{OH}] \cdot [S] \quad (1)$$

135 From the reactions 2, 3, 5, and 7, the change of  $\cdot\text{OH}$  concentration ( $\frac{d[\cdot\text{OH}]}{dt}$ ) relies on its  
 136 generation rate from  $\text{H}_2\text{O}_2$  and  $\text{Fe}^{2+}$ , and its consumption rate reacting with  $\text{Fe}^{2+}$ , organic substance  
 137 and  $\text{H}_2\text{O}_2$  as shown below:

138  
 139 
$$\frac{d[\cdot\text{OH}]}{dt} = k_2[\text{Fe}^{2+}] \cdot [\text{H}_2\text{O}_2] - k_3[\text{Fe}^{2+}] \cdot [\cdot\text{OH}] - k_5[\cdot\text{OH}][S] - k_7[\cdot\text{OH}][\text{H}_2\text{O}_2] \quad (1a)$$
  
 140

141 Since  $k_7$  ( $3.30 \times 10^7$ ) is about one order smaller than  $k_3$  ( $3.20 \times 10^8$ ) at pH 3-4 according to the  
 142 data in the literature (Dueterberg and Waite, 2006) and also  $[\text{H}_2\text{O}_2]$  is much lower than  $[\text{Fe}^{2+}]$  in  
 143 our E-Fenton reaction system, it is fair enough to remove the item of  $k_7[\cdot\text{OH}][\text{H}_2\text{O}_2]$  from Eq. 1a in  
 144 order to simplify the model.

145 Also, since  $\cdot\text{OH}$  is a highly-reactive free radical with an extremely-short lifetime of  
 146 nanoseconds (Liu et al., 1999), its concentration is normally considered to be constant but at a low  
 147 level and the  $\frac{d[\cdot\text{OH}]}{dt}$  will approach zero according to a steady state approximation. Then Eq. 1 can  
 148 be rearranged as Eq. 2 and the rate of organic degradation becomes a function of  $[\text{H}_2\text{O}_2]$  and  $[\text{S}]$   
 149 mainly.

$$150 \quad -\frac{d[\text{S}]}{dt} = k_5 \cdot \frac{k_2[\text{Fe}^{2+}] \cdot [\text{S}]}{k_3[\text{Fe}^{2+}] + k_5[\text{S}]} \cdot [\text{H}_2\text{O}_2] \quad (2)$$

151 On the other hand, the variation of  $\text{H}_2\text{O}_2$  concentration in the reaction solution depends on its  
 152 generation rate (Reaction 1) and decomposition rate (Reactions 2, 4, 6 and 7). If it is assumed that  
 153 the rate of  $\text{H}_2\text{O}_2$  generation is proportional to the applied current density ( $I/A$ ) and the oxygen  
 154 coverage ( $\theta$ ) on the cathode, it can be expressed by Eq. 3.

$$155 \quad \frac{d[\text{H}_2\text{O}_2]}{dt} = k_1 \cdot \frac{I \cdot \theta}{A} - (k_2[\text{Fe}^{2+}] + k_4[\text{Fe}^{3+}]) \cdot [\text{H}_2\text{O}_2] - k_6[\text{H}_2\text{O}_2] \cdot [\text{S}] - k_7[\cdot\text{OH}] \cdot [\text{H}_2\text{O}_2] \quad (3)$$

156  
 157  
 158 By considering that the adsorption of dissolved oxygen on the cathode surface obeys the  
 159 Langmuir adsorption model, a relationship between oxygen coverage ( $\theta$ ) and dissolved oxygen  
 160 concentration ( $[\text{O}_2]$ ) can be expressed by the following equation, where  $K_{ad}$  is the adsorption  
 161 equilibrium constant.

$$162 \quad \theta = \frac{K_{ad}[\text{O}_2]}{1 + K_{ad}[\text{O}_2]}$$

163  
 164  
 165 Since  $k_2 \gg k_4, k_6$  and  $k_7$ , Eq. 3 can be simplified into Eq. 4. After integration, the  $[\text{H}_2\text{O}_2]$   
 166 becomes a function of experimental time ( $t$ ). According to the initial condition when  $t = 0$ ,  $[\text{H}_2\text{O}_2] =$   
 167  $0$ , and also assuming that the  $[\text{Fe}^{2+}]$  during the reaction is proportional to its initial concentration  
 168 ( $[\text{Fe}^{2+}]_0$ ) with a fixed ratio of  $\lambda$ ,  $[\text{H}_2\text{O}_2]$  can be eventually expressed as Eq. 5.

$$169 \quad \frac{d[\text{H}_2\text{O}_2]}{dt} = k_1 \cdot \frac{Ik_{ad}[\text{O}_2]}{A(1 + k_{ad}[\text{O}_2])} - k_2[\text{Fe}^{2+}] \cdot [\text{H}_2\text{O}_2] \quad (4)$$

171

$$[H_2O_2] = \frac{k_1 K_{ad} I [O_2]}{k_2 \lambda A [Fe^{2+}]_0 (1 + K_{ad} [O_2])} (1 - e^{-k_2 \lambda [Fe^{2+}]_0 t}) \quad (5)$$

173

174 The above equation indicates that the  $[H_2O_2]$  is a function of experimental time, increasing  
 175 from zero at the beginning of reaction ( $t = 0$ ) toward its maximum value after sufficient reaction  
 176 time as shown below:

177

$$[H_2O_2]_{max} = \frac{k_1 K_{ad} I [O_2]}{k_2 \lambda A [Fe^{2+}]_0 (1 + K_{ad} [O_2])} \quad (5a)$$

179

180 This equation demonstrates that  $[H_2O_2]_{max}$  in the E-Fenton reaction depends on few factors of  
 181  $I/A$ ,  $[Fe^{2+}]_0$  and  $[O_2]$ . Alternatively Eq. 5 has a simplified form as shown below:

182

$$[H_2O_2] = [H_2O_2]_{max} (1 - e^{-k_2 \lambda [Fe^{2+}]_0 t}) \quad (5b)$$

184

185 Once we use Eq. 5 to replace the  $[H_2O_2]$  in Eq. 2, the rate of organic degradation can be further  
 186 expressed as follows:

187

$$-\frac{d[S]}{dt} = \frac{k_5}{k_3 \lambda [Fe^{2+}]_0 + k_5 [S]} \cdot \frac{k_1 K_{ad} I [O_2]}{(1 + K_{ad} [O_2])} (1 - e^{-(k_2 \lambda [Fe^{2+}]_0)t}) \cdot [S] \quad (2a)$$

189

190 After integration, the organic concentration  $[S]$  becomes a function of experimental time,  
 191 decreasing from its initial concentration  $[S]_0$  at the beginning of reaction ( $t = 0$ ) gradually as  
 192 described by Eq. 6:

193

$$\ln\left(\frac{[S_0]}{[S]}\right) + \frac{k_5}{k_3 \lambda [Fe^{2+}]_0} ([S_0] - [S]) = \frac{k_1 k_5 K_{ad} I [O_2]}{k_3 \lambda A [Fe^{2+}]_0 (1 + K_{ad} [O_2])} \left( t - \frac{1 - e^{-(k_2 \lambda [Fe^{2+}]_0)t}}{k_2 \lambda [Fe^{2+}]_0} \right) \quad (6)$$

195

196 To simplify Eq. 6, let  $a = \frac{k_5}{k_3 \lambda [Fe^{2+}]_0}$ ,  $b = \frac{k_1 k_5 K_{ad} I [O_2]}{k_3 \lambda A [Fe^{2+}]_0 (1 + K_{ad} [O_2])}$  and  $c = k_2 \lambda [Fe^{2+}]_0$ , the above equation  
 197 can be re-arranged in a simplified form as shown below:

198

$$199 \quad \ln \frac{[S_0]}{[S]} + a([S_0] - [S]) = b \left( t - \frac{1 - e^{-ct}}{c} \right) \quad (6a)$$

200

201 It can be concluded that the above pair of equations (Eqs. 5 and 6) has been established as the  
 202 main kinetic model for the E-Fenton reaction to describe H<sub>2</sub>O<sub>2</sub> accumulation and organic  
 203 degradation in aqueous solution against reaction time.

204

#### 205 **4. Validation of the New Kinetic Model by Experiments**

206

207 To validate the new model for its application in an E-Fenton reaction system, three sets of  
 208 experiments were carried out in aqueous phenol solution by varying three key factors of current  
 209 density (I/A), dissolved oxygen concentration ([O<sub>2</sub>]) and ferrous ion concentration ([Fe<sup>2+</sup>]),  
 210 respectively. Each experiment with an initial phenol concentration of 1.5 × 10<sup>-4</sup> M and initial pH 2.5  
 211 lasted for up to 90 min, in which the concentrations of H<sub>2</sub>O<sub>2</sub> and phenol were determined at  
 212 different reaction intervals.

213 The H<sub>2</sub>O<sub>2</sub> model (Eq. 5b) was first validated by the above experimental data of H<sub>2</sub>O<sub>2</sub>  
 214 concentration. The fitting results are presented in Fig. 1. It can be seen clearly that the new H<sub>2</sub>O<sub>2</sub>  
 215 model can well describe the H<sub>2</sub>O<sub>2</sub> variation in all experiments. Both the experimental data and the  
 216 model simulation showed that H<sub>2</sub>O<sub>2</sub> concentration increased quickly at the initial stage of the  
 217 reaction and gradually approached to the maximum values. The experimental results in Fig. 1A and  
 218 B indicate that the higher I/A and [O<sub>2</sub>] would be beneficial to enhance the H<sub>2</sub>O<sub>2</sub> generation rate,  
 219 while the results in Fig. 1C show that the higher [Fe<sup>2+</sup>] could decompose H<sub>2</sub>O<sub>2</sub> faster. These  
 220 experimental data were also fitted using Eq. 5 to demonstrate the relationship between [H<sub>2</sub>O<sub>2</sub>]<sub>max</sub>  
 221 and three factors of current density, dissolved oxygen concentration and initial ferrous ion  
 222 concentration, respectively as shown in Fig. 2. The fitting results demonstrated a good agreement  
 223 between simulation and experimental data with three correlation coefficients of R = 0.9978, 0.9973,



224 and 0.9647.

225

226 [Fig. 1]

227 [Fig. 2]

228

229 The new organic degradation model (Eq. 6) was also validated by the above first set of  
230 experiments of phenol degradation at  $[O_2] = 0.57$  mM,  $[Fe^{2+}]_0 = 0.20$  mM and pH 2.5, but three  
231 different current density ( $I/A = 0.04, 0.16$  and  $0.32$  mA cm<sup>-2</sup>). The experimental data were fitted  
232 using both the first-order model and our new model, respectively. Fig. 3 presents the results of  
233 fittings in linear forms of the first-order model (Fig. 3A) and our new model of

234  $[Ln \frac{[S_0]}{[S]} + a([S_0] - [S])]$  vs.  $(t - \frac{1 - e^{-ct}}{c})$  (Fig. 3B). It can be seen that the correlation coefficients

235 for fitting by our new model are much higher than those by the first-order model. Furthermore, Fig.

236 4 shows variation of phenol concentration  $[S]$  against reaction time (t) fitted by our new model (Eq.

237 6a). The experiments demonstrated that a trend of all experimental data between phenol

238 concentration and reaction time appeared as an inverted “S” shape curve, which means that the rate

239 of phenol degradation was quite slow during the initial stage of the reaction due to a low H<sub>2</sub>O<sub>2</sub>

240 concentration, then significantly increased during the middle stage of the reaction due to a quick

241 growth of H<sub>2</sub>O<sub>2</sub> concentration in the reaction solution, and eventually slowed down again during the

242 later stage of the reaction after phenol had been reduced to a low level. It is obvious that our new

243 model well fitted the experimental data, since the model considers both variables of phenol

244 concentration and also H<sub>2</sub>O<sub>2</sub> concentration simultaneously. Actually many reactions can not be

245 simply fitted by the first-order model. Some researchers would rather subdivide the reaction period

246 into two or three phases to fit the experimental data using the first-order model separately with

247 different values of kinetic constant (k) (Chu et al., 2005). This approach may well simulate the

248 experimental data mathematically, but not chemically. Our model can satisfy the kinetic description

249 of such an E-Fenton reaction in both ways.

250

251 [Fig. 3]

252 [Fig. 4]

253

254 It has been identified that three parameters of current density ( $I/A$ ), dissolved oxygen  
255 concentration ( $[O_2]$ ), and initial ferrous ion concentration  $[Fe^{2+}]_0$  are the key factors affecting both  
256 the  $H_2O_2$  generation and also the phenol degradation. The experimental results shown in Fig. 4  
257 demonstrated that the increase of the applied current density up to  $0.32 \text{ mA cm}^{-2}$  in the E-Fenton  
258 reaction could enhance the phenol degradation significantly, since the higher rate of  $H_2O_2$   
259 generation was achieved at the higher current density. It is believed that at the lower side of current  
260 density ( $I/A \leq 0.32 \text{ mA cm}^{-2}$ ), phenol is mainly degraded by the typical E-Fenton reaction, but at the  
261 higher side of current density ( $I/A > 0.32 \text{ mA cm}^{-2}$ ), the  $H_2O_2$  reduction to water on the cathode  
262 would be involved.

263 The experimental data from the second set of experiments with different dissolved oxygen  
264 concentration were fitted using the new model and the results are presented in Fig. 5. It can be seen  
265 that the three curves of phenol degradation at different dissolved oxygen concentration showed the  
266 same pattern of the inverted “S” shape and good fittings were achieved by our new model. Also the  
267 results showed that the higher  $[O_2]$  up to  $0.57 \text{ mM}$  accelerated the phenol degradation significantly,  
268 but not as much as the effect of current density. These results further confirmed that the rate of  
269 substance degradation can be enhanced by increasing  $I/A$  as the first-order reaction, but by  
270 increasing  $[O_2]$  at the order between 0 and 1 as indicated by Eq. 6. From an engineering point of  
271 view, the application of such an E-Fenton reaction in water and wastewater treatment should adopt a  
272 dissolved oxygen level below  $9 \text{ mg l}^{-1}$  (equivalent to  $0.28 \text{ mM}$ ), which can be simply realized by  
273 aeration under normal atmosphere pressure.

274

275 [Fig. 5]

276

277 It should be noted that the overall efficiency of phenol degradation in such an E-Fenton  
278 reaction depends on both rates of  $H_2O_2$  generation and Fenton reaction in the solution. When the  
279 current density and dissolved oxygen concentration mainly affect the rate of  $H_2O_2$  generation, the  
280 ferrous ion concentration would affect both rates of  $H_2O_2$  decomposition and  $\cdot OH$  formation in the  
281 reaction solution simultaneously. The third set of experiment of phenol degradation with different  
282 initial concentrations of ferrous ion was conducted. The results presented in Fig. 6 showed that the

283 phenol degradation reaction increased with the increased initial concentrations of ferrous ion  
284 ( $[\text{Fe}^{2+}]_0$ ) from 0.05 to 0.2 mM significantly, and further enhanced from 0.2 to 1.0 mM slightly.  
285 Without surprise, the inverted “S” shape curves of phenol concentration vs. reaction time were  
286 confirmed and the goodness of the fittings at different  $[\text{Fe}^{2+}]_0$  by our new model is presented in Fig.  
287 6.

288  
289 [Fig. 6]

290  
291 In our study, it was further found that a turning point for the enhancement of phenol  
292 degradation reaction from high to low by  $[\text{Fe}^{2+}]_0$  was around 1.0 mM under our experimental  
293 condition. At a higher  $[\text{Fe}^{2+}]_0$  of 2.0 mM, no significant increase in phenol degradation was  
294 observed. At much higher  $[\text{Fe}^{2+}]_0$ , the rate of phenol degradation could be reduced (not shown here).  
295 These results indicate clearly that there must be an optimum ferrous ion concentration in such an  
296 E-Fenton reaction. In this study,  $[\text{Fe}^{2+}]_0 = 0.2$  mM was determined to be a suitable concentration to  
297 achieve an efficient rate of phenol degradation under our experimental condition.

298  
299 Although the conventional first-order kinetic model is the simplest model to describe a variety  
300 of chemical reactions and has been widely applied in various processes relevant to water and  
301 wastewater treatment, it is difficult to well describe the kinetics of the E-Fenton reaction precisely.  
302 It should be noted that the cathodic E-Fenton reaction has a few particular characters that: (i)  $\text{H}_2\text{O}_2$   
303 is continuously generated throughout the reaction; (ii) the initial  $\text{H}_2\text{O}_2$  concentration in the reaction  
304 solution is zero and gradually increases along with the reaction time toward a maximum value,  
305 depending on the applied current density, the dissolved oxygen concentration and the ferrous iron  
306 concentration; and (iii) the variation of substrate concentration vs. reaction time has a typical  
307 inverted “S” shape curve, indicating a low reaction rate during the initial stage of the reaction, a  
308 high reaction rate during the middle stage, and a low reaction rate again during the final stage.

## 309 310 **5. Conclusion**

311  
312 In this study, a new kinetic model for the E-Fenton reaction in aqueous solution was established

313 mathematically as an analytical solution by considering both the H<sub>2</sub>O<sub>2</sub> generation rate and the H<sub>2</sub>O<sub>2</sub>  
314 consumption rate. In addition, it also includes the three key factors of current density, dissolved  
315 oxygen concentration and ferrous ion concentration. Therefore, this model with its inverted “S”  
316 shape curve can describe the cathodic E-Fenton reaction much better than the first-order model  
317 more accurately than other kinetics by subdividing the reaction period into two or three phases.  
318 However, the new model was only validated by the experiments of phenol degradation so far.  
319 Further studies to apply this kinetic model in degradation of other organics become necessary.

320

### 321 **Acknowledgements**

322 This work was financially supported by the RGC grant of Hong Kong Government (RGC Grant No.  
323 PolyU5148/03E). The project is also partially supported by Natural Science Foundation of China  
324 (Project No: 20577071) and Natural Science Foundation of China Guangdong Province, China  
325 (Project No: 04009709). The authors would thank Mr. Zhang Guangchi for his help in the  
326 modeling work.

327

### 328 **References**

- 329 Anota, J., Lu M.C., Chewprech, P., 2006. Kinetics of aniline degradation by Fenton and  
330 electro-Fenton Processes. *Wat. Res.* 40, 1841-1847.
- 331 APHA, 1995. Standard methods for the examination of water and wastewater, 19th edition.
- 332 Boye, B., Dieng, M. M., Brillas, E., 2002. Degradation of herbicide 4-chlorophenoxyacetic acid by  
333 advanced electrochemical oxidation. *Environ. Sci. Technol.* 36, 3030-3035.
- 334 Brillas, E., Baños, M. A., Garrido, J. A., 2003. Mineralization of herbicide  
335 3,6-dichloro-2-methoxybenzoic acid in aqueous medium by anodic oxidation, electro-Fenton and  
336 photoelectron-Fenton. *Electrochim. Acta.* 48, 1697-1705.
- 337 Brillas, E., Calpe, J. C., Casado, J., 2000. Mineralization of 2,4-D by advanced electrochemical  
338 oxidation process. *Wat. Res.* 34, 2253-2262.
- 339 Brillas, E., Casado, J., 2002. Aniline degradation by Electro-Fenton<sup>®</sup> and peroxy-coagulation  
340 processes using a flow reactor and for waste water treatment. *Chemosphere* 47, 241-248.
- 341 Brillas, E., Sauleda, R., Casado, J., 1998. Degradation of 4-chlorophenol by anodic oxidation,  
342 electro-Fenton, photo-electro-Fenton and peroxi-coagulation processes. *J. Electrochem. Soc.*  
343 145, 759-765.

344 Buvet, R, Sechaud, P., Darolles, J., Leport., Sechaud, F., 1987. Electrochemical and chemical  
345 reductions of oxygen dissolved in aqueous solutions. *Bioelectrochem. Bioenerg.* 18, 13-19.

346 Chu W., Kwan C. Y., Chan K. H., Kam S. K., 2005. A study of kinetic modelling and reaction  
347 pathway of 2,4-dichlorophenol transformation by photo-fenton-like oxidation. *J. Hazard. Mat.*  
348 121, 119-126.

349 Duesterberg, C. and Waite, T. D., 2006. Process optimization of Fenton oxidation using kinetic  
350 modeling. *Environ. Sci. Technol.* 40, 4189-4195

351 Gözmen, B., Oturan, M. A., Oturan, N. O., Erbatur, O., 2003. Indirect electrochemical treatment of  
352 bisphenol in water via electrochemically generated Fenton reagent. *Environ. Sci. Technol.* 37,  
353 3716-3723.

354 Joseph J. P., 1992. Dark and photoassisted Fe<sup>3+</sup>-catalyzed degradation of chlorophenoxy herbicides  
355 by hydrogen peroxide. *Environ. Sci. Technol.* 26, 944-951.

356 Kawabe, S., Kaneco, S., Suzuki, T., Ohta, K., 2004. Degradation of bisphenol A in water by the  
357 photo-Fenton reaction. *J. Photochem. Photobiol. A: Chem.* 162, 297-305.

358 Liu D. X., Liu J., Wen J., 1999. Elevation of hydrogen peroxide after spinal cord injury detected by  
359 using the Fenton reaction. *Free Radical Biology and Medicine.* 27, 478-482.

360 Liu, H., Li, F. B., Li, X. Z., 2003. Photocatalytic oxidation using a new catalyst-titanium dioxide  
361 microsphere for water and waste water treatment. *Abstr. Pap. Am Chem. S225*, PP 104.

362 Lunar, A., Sicilia, D., Rubio S., Pérez-Bendito D., Nickel, U., 2000. Degradation of photographic  
363 developers by Fenton reagent: condition optimization and kinetics for metol oxidation. *Wat.*  
364 *Res.*, 34, 1791-1802.

365 Malato, S., Caceres, J., Aguera, A., Mezcuca, M., Hernando, D., Vial, J., Fernandez-Alba, A. R.,  
366 2001. Degradation of imidacloprid in water by photo-Fenton and TiO<sub>2</sub> photocatalysis at a solar  
367 pilot plant: A comparative study. *Environ. Sci. Technol.* 35, 4359-4366.

368 Malato, S., Caceres, J., Aguera, A., Mezcuca, M., Hernando, D., Vial, J., Fernandez-Alba, A. R.,  
369 2001. Degradation of imidacloprid in water by photo-Fenton and TiO<sub>2</sub> photocatalysis at a solar  
370 pilot plant: A comparative study. *Environ. Sci. Technol.* 35, 4359-4366.

371 Neyens, E., Baeyens, J., 2003. A review of classic Fenton peroxidation as an advanced oxidation  
372 technique. *J. Haz. Mat.* 98, 33-50.

373 Oliveros, E., Legrini, O., Hohl, M., Müller, T., Braun, A. M., 1997. Industrial waste water treatment:  
374 large scale development of a light-enhanced Fenton reaction *Esther. Chem. Eng. Proc.* 36,  
375 397-405.

376 Oturan, M. A., 2000. An ecologically effective water treatment technique using electrochemically

377 generated hydroxyl radicals for in situ destruction of organic pollutants: Application to  
378 herbicide 2,4-D. *J. Appl. Electrochem.* 30, 475-482.

379 Oturan, M. A., Peiroten, J., Chartrin. P., Acher., A. J., 2000. Complete destruction of p-nitrophenol  
380 in aqueous medium by electro-Fenton method. *Environ. Sci. Technol.* 34, 3474-3479.

381 Qiang, Z. M., Chang, J. H., Huang, C. P., 2002. Electrochemical generation of hydrogen peroxide  
382 from dissolved oxygen in acidic solutions. *Wat. Res.* 36, 85-94.

383 Sellers, R.M., 1980. Spectrophotometric determination of hydrogen-peroxide using potassium  
384 titanium(IV) oxalate. *Analyst* 105, 950-954.

385 Vogel, A., 1978. *A Textbook of Quantitative Inorganic Analysis*, fourth ed. Longman Scientific and  
386 Technical, England.

387 Walling, C., 1975. Fenton Reagent Revisited. *Acc. Chem. Res.* 8, 125-131.

388 Wang, Q.Q., Lemley, A.T., 2001. Kinetic model and optimization of 2,4-D degradation by anodic  
389 Fenton treatment. *Environ. Sci. Technol.* 35, 4509-4514.

390

391 **LIST OF FIGURE CAPTIONS**

392

393 Fig. 1. H<sub>2</sub>O<sub>2</sub> accumulation in the reaction solution with initial phenol concentration of  $1.5 \times 10^{-4}$  M  
394 (A) different I/A, when  $[O_2] = 0.57$  mM and  $[Fe]_0 = 0.20$  mM; (B) different  $[Fe^{2+}]_0$ , when I/A =  
395  $0.32$  mA cm<sup>-2</sup> and  $[O_2] = 0.57$  mM; and (C) different  $[O_2]$ , when I/A =  $0.32$  mA cm<sup>-2</sup> and  $[Fe]_0$   
396 =  $0.20$  mM.

397

398 Fig. 2. Linear fittings of  $[H_2O_2]_{max}$  at different (A): I/A, (B):  $[Fe^{2+}]_0$  and (C):  $[O_2]$ , respectively.

399

400 Fig. 3. Linear relationship of phenol degradation during the E-Fenton reaction at different I/A fitted  
401 by (A) the first-order model and (B) the new kinetic model, when  $[O_2] = 0.57$  mM,  $[Fe]_0 = 0.2$   
402 mM and pH 2.5.

403

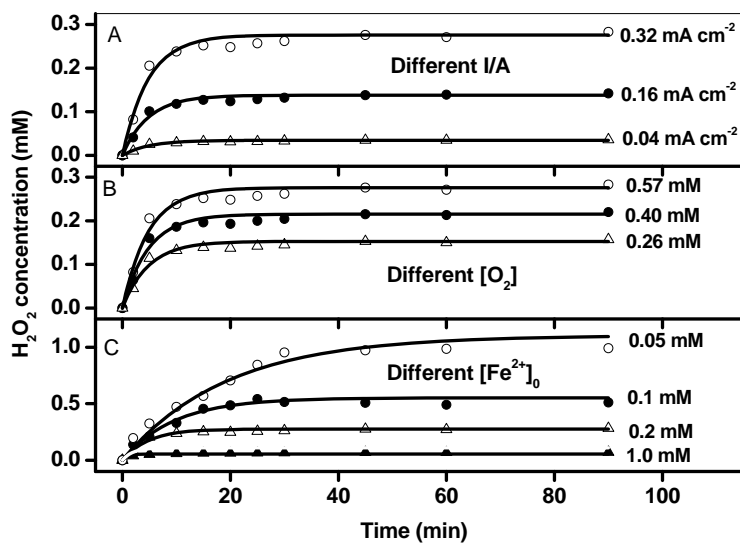
404 Fig. 4. Phenol degradation during the E-Fenton reaction at different I/A fitted by the new kinetic  
405 model ( $[O_2] = 0.57$  mM,  $[Fe]_0 = 0.2$  mM and pH 2.5).

406

407 Fig. 5. Phenol degradation during the E-Fenton reaction at different  $[O_2]_0$ , fitted by the new kinetic  
408 model ( $K_{ad} = 1.1$  L mM<sup>-1</sup>,  $k_1 = 6.6$  M<sup>-1</sup> S<sup>-1</sup>,  $k_2 = 81$  M<sup>-1</sup> S<sup>-1</sup>,  $k_5/k_3 = 0.31$ ,  $\lambda = 0.2$ , pH 2.5, I/A =  
409  $0.32$  mA cm<sup>-2</sup> and  $[Fe^{2+}]_0 = 0.2$  mM).

410

411 Fig. 6. Phenol degradation during the E-Fenton reaction at different  $[Fe^{2+}]_0$  fitted by the new kinetic  
412 model ( $K_{ad} = 1.1$  L mM<sup>-1</sup>,  $k_1 = 6.6$  M<sup>-1</sup> S<sup>-1</sup>,  $k_2 = 81$  M<sup>-1</sup> S<sup>-1</sup>,  $k_5/k_3 = 0.31$ ,  $\lambda = 0.2$ , pH 2.5, I/A =  
413  $0.32$  mA cm<sup>-2</sup> and  $[O_2]_0 = 0.57$  mM).



414

415

416

417

418

419

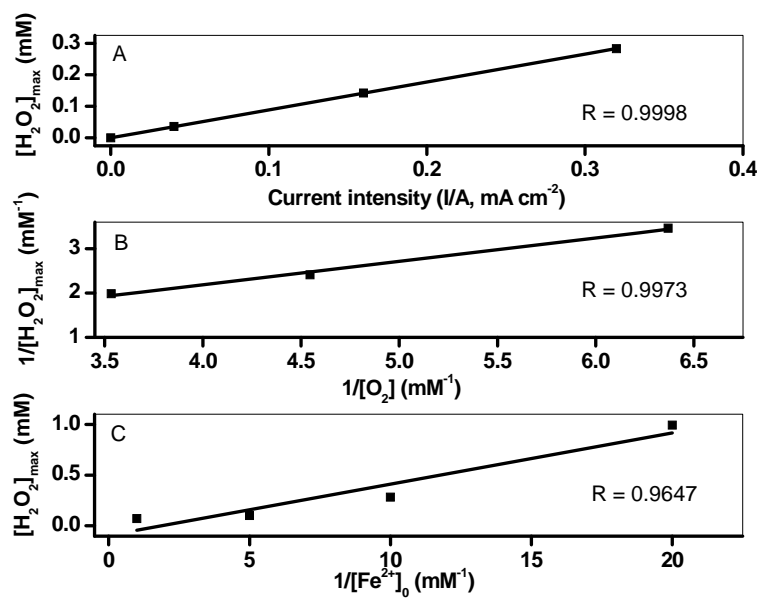
420

421

**Fig. 1.**



422



423

424

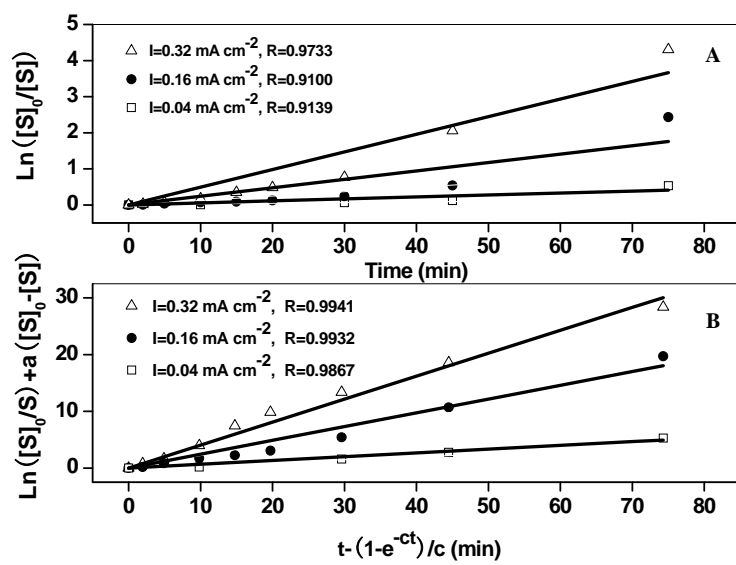
425

426

427

428

**Fig. 2.**



430

431

432

433

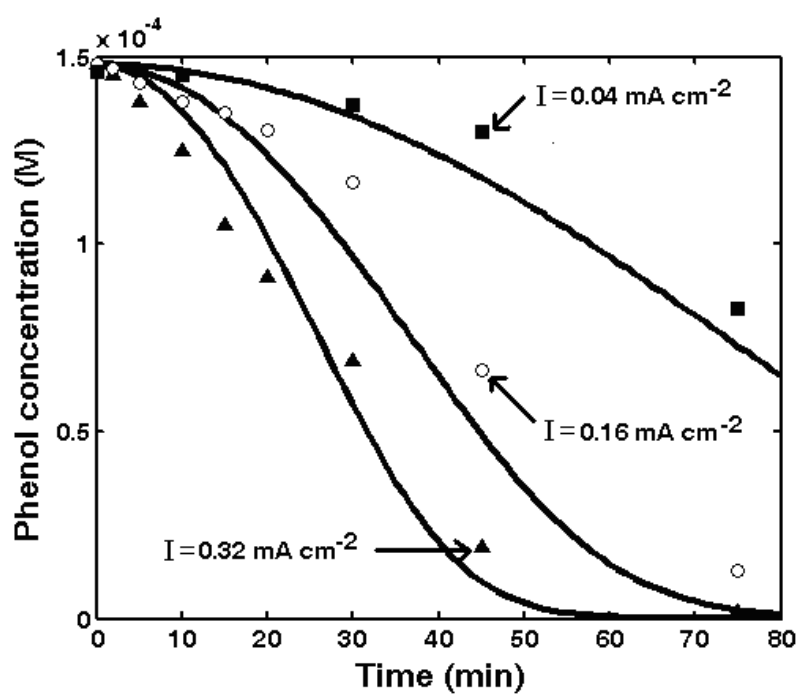
434

435

436

Fig. 3.

437



438

439

440

441

442

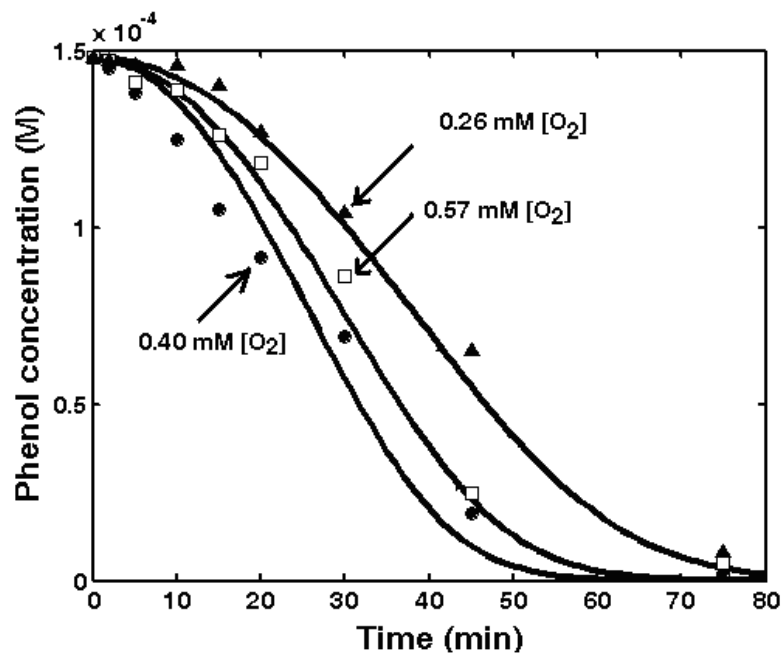
443

444

445

446

Fig. 4.



447

448

449

450

451

452

453

454

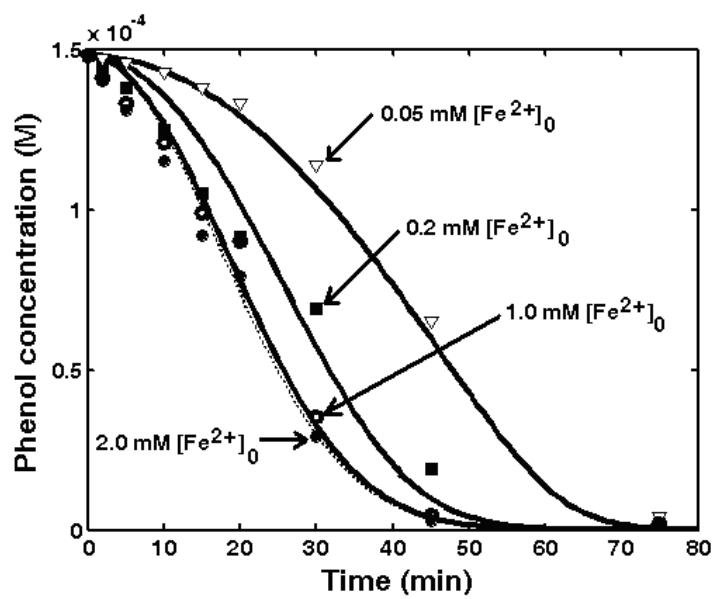
455

456

457

458

Fig. 5.



460

461

462

463

464

Fig. 6.